Journal Pre-proof

Nano-immobilization of PETase enzyme for Enhanced Polyethylene Terephthalate Biodegradation

Yunpu Jia, Nadia A. Samak, Xuemi Hao, Zheng Chen, Gama Yang, Xuhao Zhao, Tingzhen Mu, Maohua Yang, Jianmin Xing

PII: S1369-703X(21)00281-3

DOI: https://doi.org/10.1016/j.bej.2021.108205

Reference: BEJ108205

To appear in: *Biochemical Engineering Journal*

Received date: 13 June 2021
Revised date: 14 August 2021
Accepted date: 3 September 2021

Please cite this article as: Yunpu Jia, Nadia A. Samak, Xuemi Hao, Zheng Chen, Gama Yang, Xuhao Zhao, Tingzhen Mu, Maohua Yang and Jianmin Xing, Nano-immobilization of PETase enzyme for Enhanced Polyethylene Terephthalate Biodegradation, *Biochemical Engineering Journal,* (2021) doi:https://doi.org/10.1016/j.bej.2021.108205

Nano-immobilization of PETase enzyme for Enhanced Polyethylene Terephthalate Biodegradation

Yunpu Jia [a,b], Nadia A. Samak [a,b,c,e], Xuemi Hao [a,b], Zheng Chen [a,b], Gama Yang [a,b], Xuhao Zhao [a] , Tingzhen Mu [a], Maohua Yang [a], Jianmin Xing [a,b,d,*]

[a] CAS Key Laboratory of Green Process and Engineering, State Key Laboratory of Biochemical Engineering, Institute of Process Engineering, Chinese Academy of Sciences, Beijing 100190, PR China

[b] College of Chemical Engineering, University of Chinese Academy of Sciences, Beijing 100049, PR China

[c] Environmental microbiology and biotechnology, Aquatic microbiology, University of Duisburg-Essen, 4141 Essen, Germany

[d] Chemistry and Chemical Engineering Guangdong Laboratory, Shantou 515031, P. R. China

[e] Processes Design and Development Department, Egyptian Petroleum Research Institute, Nasr City, 11727 Cairo, Egypt

* Corresponding author at: CAS Key Laboratory of Green Process and Engineering& State Key Laboratory of Biochemical Engineering, Institute of Process Engineering, Chinese Academy of Sciences, 1, Zhongguancun Bei-er-tiao, Haidian District, Beijing 100190, PR China. E-mail address: jmxing@ipe.ac.cn.

ABSTRACT

PET hydrolase (PETase), discovered in *Ideonella sakaiensis*, is a promising agent for the biodegradation of polyethylene terephthalate (PET) capable of PET decomposition under mild reaction conditions with limited stability and productivity. Here, the immobilization of His-tagged PETase was achieved by synthesizing

enzyme-inorganic nanoflowers, PETase@$Co_3(PO_4)_2$, which was designed based on the principle of biomimetic mineralization. Immobilization of PETase onto nanostructured $Co_3(PO_4)_2$ enjoys high enzyme loading and low mass transfer inhibition due to large specific surface area, high movement speed, and large surface curvature caused by small particle size. The nano-effect of inorganic carriers materialize the 10°C optimum temperature swelling of the immobilized PETase with enhanced pH tolerance (6.0-10.0) than the free counterpart. The long-duration reaction showed that the productivity of terephthalic acid (TPA) was 3.5 times higher than that of the free enzyme. PETase@$Co_3(PO_4)_2$ still retained 75% of the initial activity after 12 days compared with the free enzymes, which showed almost no activity. The excellent and stable catalytic performance of PETase@$Co_3(PO_4)_2$ with low cost demonstrates the synthetical usefulness of immobilization via biomimetic mineralization in the enzyme utilization in industrial PET depolymerization.

Keywords:

Plastic biodegradation; Immobilization of biocatalyst; Biomimetic mineralization

1. Introduction

Plastics have been massively produced over the past few decades and become essential to modern society, driven by their durability, plasticity, and chemical stability. However, poor management and disposal methods engendered explosive

accumulation worldwide [1]. The environmental threat of plastic pollution, especially in marine ecosystems, is further recognized for the ultra-long lifetimes of plastics [2-4]. Especially for PET, with only two simple monomers, TPA and ethylene glycol (EG), connected by an ester bond, is relatively solid and difficult to degrade naturally. The current treatment methods of PET waste like recycling, landfill treatment, and incineration treatment, have apparent limitations, for example, the considerable investment in PET recycling, land pollution causing by landfill treatment, and air pollution resulting from incineration.

Biodegradation has been considered an effective method to control PET pollution profit for its eco-friendly and cost-effective characteristics [4-6]. The biodegradation of PET could be performed by the whole-cell organism or by the produced enzymes. Several enzymes that catalyze PET hydrolysis have been discovered in the past few years and identified as promising and environmental biocatalysts to alternate chemical or physical recycling [7-12]. For example, after extracting the cutinase named LCC from a fosmid library of a leaf-branch compost metagenome [12], Tournier et al. improved its hydrolysis capacity that ultimately achieved a minimum of 90% PET depolymerization into monomers over 10 hours [10]. Polyester hydrolase TfCut2 from *Thermobifida fusca* KW3 is another candidate with a high-PET hydrolytic activity [11]. Roth and his co-workers [13] structurally characterized TfCut2 and proposed a model for the binding of the enzyme towards its polymeric substrate. In 2016, a PET-specific hydrolase named PETase (EC: 3.1.1.101, PDBID:5XJH),

identified from bacterium *Ideonella sakaiensis* strain 201-F6, exhibits high depolymerization activity against PET films under mild reaction conditions [14]. However, its instability during the long-term storage and plastic depolymerization process hinders its application in industrial large-scale PET biodegradation.

Immobilization of PETase using the facile methods is a suitable solution to the abovementioned problems. In the past few decades, immobilized enzymes influenced by carrier choices have demonstrated superior performance due to their higher stability, better reusability, and easier separation from the reaction mixture than their free forms [15]. Traditional immobilization approaches mainly include three groups, binding to supports, carrier-free insolubilized enzyme aggregates, and entrapment in polymer materials [31]. Compared with traditional materials, nanostructures can stabilize enzymes for a long time in different systems with nano-effects such as the small size and the large surface curvature of the nanoparticles [16].

Recently, the biomimetic mineralization process has caught many eyeballs with its ease operation, ultrahigh enzyme activity recovery rate, mild reaction conditions, and the specially enhanced stabilization effect of enzyme−inorganic hybrid nanoflowers on enzymes component [17]. Unlike any traditional immobilization method, the biomimetic mineralization process is a new immobilized enzyme technology accompanied by inorganic salt precipitation. A low-concentration buffer is used to slow down the rate of inorganic salt formation, with enzyme molecules introduced in the reaction to allow inorganic salt precipitation to adhere to the enzyme

slowly [24]. Then, embedding was carried out to immobilize of the enzyme. The method utilizes the specific chelation of the imidazole group in his-tag exposed on the protein surface and metal ions to immobilize the protein, whose affinity then be purified. The inorganic nanoparticles as carriers reduced the steric hindrance and substrate diffusion limiting. Following the protein-inorganic ($Cu_3(PO_4)_2$) hybrid system by Ge et al. [18], and subsequently, some scientists synthesized several other hybrid nanoflowers using different inorganic or organic components for the efficient immobilization of hydratase, lipase and transaminase [19-21]. Encouraged by these early achievements, a biomimetic mineralization strategy that introduces an affinity tag at the N-terminal of the PETase to realize the purification and immobilization of the enzyme was adopted. PETase flower-like cobalt phosphate nanoparticles were produced by the nucleation reaction of the cobalt ions and PETase enzyme that was assembled on the surface of particles. Catalytic activities and stabilities of the free and immobilized PETase toward PET films were studied. The reusability efficiency and storage performance of the immobilized PETase enzyme were also examined.

2. EXPERIMENTAL

2.1. Materials

The complete gene sequence of PETase from *Ideonella sakaiensis* strain 201-F6 (Genbank GAP38373.1) was codon-optimized and synthesized, then inserted into the target vector pET-30a (+) for the expression in *Escherichia coli* BL21 (DE3). For immobilized PETase, a 6xHis tag was added into the N-terminal of its sequence. The

sequence of the resulting plasmids was confirmed using Sanger sequencing at GenScript China, Inc. Acetonitrile (HPLC grade) was purchased from Shanghai Macklin Biochemical Co., Ltd. (China). All other chemicals of analytical grade were purchased from Sigma-Aldrich Trading Co. Ltd. (Shanghai, China) unless otherwise stated.

2.2. Preparation of PETase@$Co_3(PO_4)_2$.

2.2.1. Expression and purification of His-tagged PETase.

The recombinant plasmid pET-30a(+) (**Scheme S1**) carrying the His-tagged PETase gene was transformed to *E. coli* BL21 (DE3) cells. Successful transformants were cultured overnight (1%, v/v) in 50 mL Luria-Bertani (LB) medium containing 50 mg/L kanamycin at 37 °C. 0.6 mM isopropyl-β-D-thiogalactopyranoside (IPTG) was added to induce the His-tagged PETase expression after the culture OD_{600} value reached 2.4. After induction at 21 °C for 36 h, the mixture was centrifuged for 5 minutes at 4 °C. The collected cells were resuspended in a Lysis buffer composed of sodium phosphate (20 mM), imidazole (20 mM), and NaCl (0.5 M) with pH 7.4. After that, the resuspended cells were disrupted by an ultrasonic homogenizer at 4 °C. The lysate containing the PETase enzyme, was collected via centrifugation at 4 °C for 20 min after sonication. Subsequently, the clear lysate was loaded onto the His-tagged nickel column (Cytiva, America) for purification. A wash buffer (sodium phosphate (20 mM), imidazole (20 mM), NaCl (0.5 M), pH 7.4) was used to wash the column. Elution buffer (sodium phosphate (20 mM), imidazole (500 mM), NaCl (0.5 M), pH

7.4) was used to elute the bound proteins. The purification process was conducted according to the previous literature [22]. Sodium dodecyl sulfate polyacrylamide gel electrophoresis (SDS-PAGE) checked the purity of the purified PETase enzyme.

2.2.2. Preparation of cobaltous phosphate nanoparticles.

Cobaltous phosphate nanoparticles were synthesized according to the previous reports [21]. Briefly, $Co(NO_3)_2 \cdot 6H_2O$ was added to 10 mM phosphate-buffered saline (PBS) solution (10 mM, pH 7.4) with 10 mM Co^{2+} as a final concentration. After complete oscillation, the mixture turned purple and pink floccules began to appear. Subsequently, the mixture was incubated for 36 h at room temperature. After washing 3 times using ultrapure water, the cobaltous phosphate nanoparticles were obtained by suspension with a certain amount of ultrapure water.

2.2.3. Preparation of PETase-inorganic hybrid nanoflowers.

PETase@$Co_3(PO_4)_2$ nanoflowers were synthesized by mixing crude enzyme (10 mL), PBS (90 mL, 10 mM), and $Co(NO_3)_2 \cdot 6H_2O$ (0.291 g), then incubated at 25 °C for 60 h. After that, they were collected by 3 cycles of centrifugation (6500 rpm) for 5 min, and subsequently, the produced nanoflowers were washed with ultrapure water.

2.2.4. Tryptophan fluorescence emission of PETase-inorganic hybrid nanoflowers and free PETase.

The free PETase and PETase-inorganic hybrid nanoflowers were characterized by tryptophan fluorescence measurements. The fluorescence spectrum was recorded at the same enzyme concentration. The excitation wavelength was 230 nm and emission

fluorescence were measured from 280 nm to 600 nm using Microplate Reader (Infinite M200, Tecan Japan Co., Ltd., Kawasaki, Japan).

2.3. Enzyme Activity Assay.

2.3.1 Enzyme assays for 4-nitrophenyl butyrate.

A mixture of 49 mL phosphate buffer (100 mM, pH 7.5) and 1 mL of p-nitrophenyl butyrate(p-NPB) stock solution (4 mM, 0.084 g in absolute ethanol) was reacted well, then 50 μL of the enzyme solution was added to a cuvette containing 1 mL of p-NPB solution and mixed by pipetting. The absorbance at 400 nm was measured at 35 ℃ using HITACHI U-2910 spectrophotometer (Japan) with a measured absorbance that can be availed to calculate units of lipase activity (U) according to Eq. 1. One unit of PETase activity was defined as the amount of enzyme required to hydrolyze 1 μmol of substrate per minute [32]. For the activity measurement of the enzyme, the final enzyme activity (U_{final}) is defined as the absorbance change caused by the addition of enzyme minus the absorbance change caused by the same reaction system without enzyme. In case of PETase@$Co_3(PO_4)_2$, the final enzyme activity is defined as the absorbance change caused by the addition of the enzyme minus the absorbance change caused by the reaction system with the same concentration of $Co_3(PO_4)_2$ (Eq. 2).

$$U_{enzyme} = \frac{(A_{400nm}(t_1) - A_{400nm}(t_0)) \times V_{total}}{\varepsilon \times V_{enzyme} \times (t_1 - t_0) \times l} \quad \text{Eq. 1}$$

$A_{400nm}(t_1)$= absorbance at 400 nm measured after the enzymatic reaction is finished

$A_{400nm}(t_0)$= absorbance at 400 nm measured before the enzymatic reaction is

started

t_1 = time point when the reaction is finished

t_0 = time point when the reaction is started, usually 0 min

V_{total} = volume of reaction sample plus enzyme sample (V_{enzyme})

ε = molar extinction coefficient [mmol^{-1} dm^3 cm^{-1}]

l = light path length [cm]

$$U_{final} = U_{enzyme} - U_{control} \quad \text{Eq. 2}$$

$U_{control}$ = activity of inorganic components or reaction buffer

2.3.2 Optimum Temperature and pH

The free and immobilized PETase were incubated for 1 h in acetate buffer (pH 4-6), phosphate buffer (pH 7.0 - 10.0), or borate buffer (pH 10 - 12) with different pH values and at different temperatures (20 - 60 °C). The 100% maximum activity or initial activity was followed by the relative activity results.

2.3.3 Stability and reusability assay

Thermal stability of the immobilized PETase@$Co_3(PO_4)_2$ and free PETase were studied. Samples were incubated in Tris-HCl buffer (pH 8.0, 50 mM) for 30 minutes at 40 or 45 °C, separately with the pH stabilities of the immobilized PETase@$Co_3(PO_4)_2$ and PETase investigated by incubating them in phosphate (pH 10.0, 50 mM) or acetate buffer (pH 4.0, 50 mM) at room temperature over different time intervals. Then, their residual activity to 4-nitrophenyl butyrate was measured.

Reusability of PETase@$Co_3(PO_4)_2$ nanoflowers were studied for ten cycles by

hydrolyzing 4-nitrophenyl butyrate during repeated usages at optimized conditions. After each catalytic cycle of reaction, the immobilized enzymes were collected by centrifugation, washed twice, and resuspended using phosphate buffer (50 mM, pH 7.5) three times for the next reaction. The catalytic activity in the first cycle was defined as 100%.

2.3.4. Enzyme assays for highly crystallized PET (hcPET).

PET from a conventional bottle (NONGFU SPRING, 2 L, specific polymer characteristics unspecified) was cut into small pieces of 0.017 g about 1 cm^2 square in area. The 5 mL unpurified crude enzyme from 100 ml of cell culture was reacted with PET film in 30 mL of buffer containing 50 mM Na_2HPO_4-HCl (pH 8.0). Controls were performed using buffer or buffer containing $Co_3(PO_4)_2$ without enzyme. The experiment was stopped by removing the PET fragments from the flasks. After washing and drying, PET films were processed for scanning electron microscopy (SEM) analysis as following: the enzyme-treated PET films were washed successively with 1% SDS, ultrapure water, and ethanol. Finally, the PET film was dried before coated with Au, and Field Emission Scanning Electron Microscopy (FE-SEM) observed the degradation with a JSM-7800 or a JSM-6700F (Japan Electronics).

2.3.5. Enzyme assays for amorphous PET films and PET powder degradation.

The materials used to test PET degradation products were PET powder and amorphous PET films purchased from Goodfellow GmbH (Product number 048-768-25 and product number 029-198-54, separately). The 5 mL unpurified crude enzyme (or 5 mL nanoflowers solution with the same enzyme concentration) was incubated

with 0.15 g amorphous PET films and 0.2 g PET powder in a 30 mL total reaction system, with the reaction processes the same as that in section **2.3.4.** The degradation products were measured by High-performance liquid chromatography, HPLC (Agilent Technologies).

2.4 Synthesis of MHET substrate

Mono(2-hydroxyethyl) terephthalate (MHET) was synthesized from the hydrolysis of bis(2-hydroxyethyl) terephthalate (BHET) with KOH. Briefly, 2 g (8.74 mmol) BHET was reacted with 0.42 g (8.4 mmol) KOH in 20 g $MgSO_4$-dried and filtered ethylene glycol for 2.5 h at 110 -130 °C. The mixture of the 30 mL H_2O and the reaction system was extracted three times with 3-5 mL CH_2Cl_2 with the CH_2Cl_2-phase discarded. The precipitation of MHET was on the heels of the aqueous phase pH adjusted to 3 with 25% hydrochloric acid (HCl). The extraction procedure was conducted with 30 mL boiled water with three times filtration at 4 °C and dried precipitation at 60 °C.

2.5 HPLC analysis.

The degradation products such as MHET, TPA and BHET were separated using HPLC with the aid of C18 column on an Agilent 1200 LC system with a G1315D diode array detector (DAD). Samples and standards were injected at a volume of 20 μL onto a ChromCore C18 column 5 μm, 4.6 × 250 mm column (NanoChrom, China). A mixture of 0.1% (v/v) formic acid (A) and acetonitrile (B) was used as the mobile phase at a flow rate of 0.8 mL min^{-1} to separate the analytes of interest. The mobile phase B was changed gradually from 1 to 5% for 5 min, 5 to 44% for 7 min,

44 to 70% for 3 min, with the constant ratio for 10 minutes. The concentration of TPA, MHET and BHET was detected at a wavelength of 241 nm and quantified from the areas of the absorption peaks by standard curves.

3. Results and discussion

3.1 Specificity of cobalt phosphate to His-Tagged PETase from cell Lysates.

Cell lysates containing PETase were mixed directly with $Co(NO_3)_2$ and PBS solution without any purification process to prepare PETase@$Co_3(PO_4)_2$. Ni-NTA column witnessed the unsatisfactory effect in the enzyme purification, as shown in **Fig. 1**, lane 2. This may be attributed to Ni^{2+} can bind to some non-His-tagged proteins, resulting in poor selectivity and affecting the purification effect[33, 34]. In contrast, Co^{2+} enjoys a higher purity target protein with the weaker non-specific binding ability to His-tagged proteins [35].To verify the selectivity of the immobilization process, SDS-PAGE was used to analyze PETase purity and concentration with the molecular weight of PETase, 29 kDa, according to the calculation. The intense band between 28 and 38 kDa in line 3 (**Fig. 1**) elucidated that the used method efficiently enriched and purified the His-tagged PETase from the crude enzyme when compared with the conventional one.

3.2 Characterization of the immobilized PETase@$Co_3(PO_4)_2$.

The biomimetic mineralization process of PETase and $Co_3(PO_4)_2$ was initiated by the Co^{2+} - protein molecules complexes[18] through the coordination facility of amide groups in the protein backbone[23]. SEM images showed that cobalt phosphate

crystals had a unique flower-like shape and an elegant structure with a diameter of about 10 μm (**Fig. 2a**). Unlike $Co_3(PO_4)_2$ nanoflowers, the rough surface morphology of PETase@$Co_3(PO_4)_2$ with a beautiful rose-like structure and a diameter of about 10 μm was rough due to the incorporation of PETase enzyme (**Fig. 2b**). Furthermore, the visibly aggregated enzyme particles on the nanoflowers indicated a successful bond between PETase and the $Co_3(PO_4)_2$ crystals.

Tryptophan, an important intrinsic fluorescent, can be used to estimate the nature of the tryptophan microenvironment. Tryptophan fluorescence emission experiments studies revealed the differences in structural rearrangements of the enzyme. Compared with the free PETase, cobalt phosphate mineralization caused a λ_{max} blue shift in PETase, with significant swelling of the fluorescence intensity (**Fig. 3**). This phenomenon is attributed to the significantly altered polar environment of the aromatic residues (phenylalanine and tryptophan, Phe and Trp) caused by cobalt phosphate molecules. These alterations indicate essential changes in the tertiary structure of PETase as it formed part of cobalt phosphate biological mineral [24]. However, the preservation of the catalytic properties of the soluble PETase in enzyme may be due to the void critical domains of catalysis in the nucleation points.

Meanwhile, the PETase@$Co_3(PO_4)_2$ nanoflowers were characterized by X-ray Diffraction (XRD) (**Fig. S1**). The pleasant match between the result and the diffraction standard card for $Co_3(PO_4)_2 \cdot 8H_2O$ (JCPDS file no. 410375) indicated that the incorporation of the PETase did not affect the crystal morphology of $Co_3(PO_4)_2$.

Additionally, the surface functional groups of $Co_3(PO_4)_2$ and PETase@$Co_3(PO_4)_2$ were characterized by Fourier transform infrared (FT-IR) spectrometry. The peak at 1550 cm^{-1}, 1750 $cm^{-1,}$ 2971 cm^{-1}, and 3321 cm^{-1} corresponding to the −NH bending vibration, −C−N stretching vibration, $-CH_3$ stretching vibration, and N-H stretching vibration (**Fig. S2)**, are considered as different characteristic absorption peaks that were invisible in $Co_3(PO_4)_2$. Furthermore, Thermogravimetric Analysis (TGA) was also conducted to verify the existence of the PETase in nanoflowers. As shown in **Fig. S3**, the two samples with different relative gravities decomposed starts from 100 °C and finished around 170 °C, resulting in crystalline water loss. The extra weight loss from 200 to 400 °C in PETase@$Co_3(PO_4)_2$ as the PETase decomposed further elucidated the immobilization of PETase in PETase@$Co_3(PO_4)_2$.

X-ray photoelectron spectroscopy (XPS) was performed to investigate the surface element composition and chemical bonds of PETase@$Co_3(PO_4)_2$, whose survey scan displayed five characteristic peaks at 782, 531, 400, 285 and 134 eV, with their corresponding to Co, O, N, C and P, respectively (**Fig. S4)** suggesting the organic-inorganic hybrids of particles. Then, high-resolution XPS spectra were obtained for Co, O, and C, chimed with the previous literature[20]. The N_2 adsorption-desorption isotherms for both PETase@$Co_3(PO_4)_2$ and $Co_3(PO_4)_2$ nanoflowers were type III curves (**Fig. S5**), which indicated that the holes in the materials are slit holes formed by accumulated of flake particles[25]. The pore-size distribution plot was calculated by the Barrett-Joyner-Halenda (BJH) absorption method, revealed the average pore

size of $Co_3(PO_4)_2$ and PETase@ $Co_3(PO_4)_2$ 15.1 nm and 16.0 nm, respectively. The specific surface area and cumulative volume of pores were 32.5 m^2g^{-1} and 0.13 cm^3g^{-1} for $Co_3(PO_4)_2$, and 42.4 m^2g^{-1} and 0.17 cm^3g^{-1} for PETase@ $Co_3(PO_4)_2$, respectively. The variation of these parameters of PETase@$Co_3(PO_4)_2$ compared with $Co_3(PO_4)_2$ confirmed the successful immobilization of PETase.

3.3 Optimum Temperature and pH.

The effects of temperature and pH on the activity of PETase and immobilized PETase@$Co_3(PO_4)_2$ were investigated. **Fig. 4a** indicated the optimum pH for both free PETase and immobilized PETase@$Co_3(PO_4)_2$, 7.0, with PETase@$Co_3(PO_4)_2$ surprisedly presenting a more extensive pH range of 6.0-10.0 than that of free PETase. The biomineral surface could buffer the microenvironment near PETase by maintaining neutral pH even under extreme pH conditions[26]. The optimum temperature of the immobilized PETase@$Co_3(PO_4)_2$, 45 °C, was 10 °C higher than that of the free enzyme. The shifted of the optimum temperature and pH indicated the higher tolerance of the PETase@$Co_3(PO_4)_2$ towards changed of temperature and pH with more excellent stability than its free form. These phenomena might be ascribed to the specific His-tags affinity to Co^{2+} that failed to affect protein stability with favorable changes in secondary structure, climbed PETase rigidity, and protection on the conformation of PETase during extreme environmental conditions. The maximum enzyme activity of PETase@$Co_3(PO_4)_2$ and free enzyme measured under optimal temperature and pH conditions were 4102 U/mL and 4411 U/mL respectively. The

higher steric hindrance between the immobilized PETase and the substrate than that of the free enzyme led to the slightly lower enzyme activity of the immobilized enzyme than that of the free one [30].

3.4 Stability and Reusability assay.

The reaction rate usually increases as temperature climbs within a specific range, but higher temperature values can quickly destroy the structure and active site of the enzyme. Therefore, its ability to resist high temperatures is a crucial parameter for performance evaluation of the immobilized enzyme. **Fig. 4c** showed the thermal stabilities of free and immobilized PETase. After being incubated at 40 °C for 3 h, the immobilized PETase@$Co_3(PO_4)_2$ still held 94.4% primary activity while the free PETase kept 57.3% only. After incubation at 45 °C for 3 h, the residual activity of free PETase maintained 17.2% primary activity, compared to 82.8% for the immobilized PETase@$Co_3(PO_4)_2$. The pH stability results of free PETase and immobilized PETase@$Co_3(PO_4)_2$ are shown in **Fig. 4d**. At pH values of 4.0 and 10.0, the activity of free enzymes was dropped sharply compared with that after 5 h of incubation. In contrast, the PETase@$Co_3(PO_4)_2$ retained 67.6% of the original activity at pH 10.0 and 62.3% at pH 4.0 after incubation for 4 h. Clearly, PETase@$Co_3(PO_4)_2$ showed significant improvement in thermal stability and pH tolerance of the enzyme compared to that of the free PETase. The limitedly maintained enzyme structure by the high nanopore curvature stably immobilized the enzyme, keeping high catalytic activity even in extreme environments [27].

To test the storage stability, free PETase or immobilized PETase@$Co_3(PO_4)_2$ nanoflowers were incubated in PBS solution at room temperature. **Fig.5** indicated that the immobilized PETase@$Co_3(PO_4)_2$ only decreased 25% of its residual activity after storage at room temperature for 12 days compared with the almost inactive free enzymes. For the reusability, PETase nanoparticles minimizing alterations in structure and enzyme active sites enabled 70.2% retained residual activity to 4-nitrophenyl butyrate of the immobilized PETase@$Co_3(PO_4)_2$ after 10 cycles of use [17].

In order to compare the degradation ability of PETase@$Co_3(PO_4)_2$ and free PETase on PET, post-consumed bottle-grade PET was used as the substrate. The PET degradation reaction was terminated by removing the PET material from the enzymatic decomposition reaction system after 48 h at 35 °C with the PET films washed and dried, and their surface morphology examined by SEM (**Fig. 6**). The control group, without any enzyme, did not induce any detectable change for the PET substrate surface morphology, whereas the free PETase caused grooves and folds, chiming with the previously reported literature[14, 22, 28, 29]. Surprisingly, PETase@$Co_3(PO_4)_2$ could cause more severe erosion on the PET surface than the free PETase with obviously eroded PET film surface. To achieve the same degradation effect as PETase@$Co_3(PO_4)_2$, free PETase needed a more prolonged time, as shown in **Fig. 6e**, that slowly decreased the free PETase activity until it was lost. On the other hand, the immobilized PETase@$Co_3(PO_4)_2$ with high activity was consistent with the previous results shown in **Fig. 5**. The discovered enzyme image attached to the PET

surface with a degradation reaction marked the occurred degradation. (**Fig. S6**).

The degradation products were analyzed with PET particles and amorphous PET film as the substrate, as indicated in **Fig. 7**. The amorphous PET film or PET particles was incubated separately with the PETase@$Co_3(PO_4)_2$ nanoflowers and free PETase at 35 °C for 7 days. The absorption peaks of TPA, MHET and BHET at 241 nm were measured after dilution (**Fig. S7**). **Fig. 7** shows more degradation products in PETase@$Co_3(PO_4)_2$ than the free enzyme after 48 h with 3.5 times higher total equivalent TPA than the free enzyme. The calculated PET loss is 0.0517 g and 0.0147 g, corresponding to 25.8 % and 7.4% of the original weight, respectively. Similarly, when PET film is used as the substrate, the weight loss is 21.8 % and 7.7% of the original weight, respectively. Therefore, PETase@$Co_3(PO_4)_2$ had more robust enzymatic activity than free PETase in long-term degradation experiments. The active conformation of the immobilized PETase significantly improved its catalytic activity and stability. In addition, compared with the amorphous PET film, the better degradation effect on the PET particles of both enzyme samples could be attributed to the smaller specific surface area of the particles, easier to diffuse to the surface of the enzyme.

4. Conclusions

In summary, the facile and efficient biomimetic mineralization process witnessed the effective immobilization of the PETase into the $Co_3(PO_4)_2$ nanoflower at room

temperature. Based on the strong affinity interaction between the His-tag located on PETase and cobaltous phosphate, the oriented purification and immobilization of PETase from crude enzyme without pre-purification has been realized. Owing to the unique structure, the hybrid nanoflowers biocatalyst (PETase@$Co_3(PO_4)_2$) showed significantly higher catalytic efficiencies and stability. The obtained nanocatalyst provides valuable information for achieving efficient applications in the biodegradation of PET.

Acknowledgment

The authors gratefully acknowledge the financial support provided by the National Natural Science Foundation of China (grant numbers 31961133017, 31961133018, 31961133019). These grants are part of "MIXed plastics biodegradation and UPcycling using microbial communities" MIX-UP research project, which is a joint NSFC and EU H2020 collaboration. In Europe, MIX-UP has received funding from the European Union's Horizon 2020 research and innovation program under grant agreement No 870294.

Appendix A. Supplementary data

Supplementary material related to this article can be found online at

References

[1] R. Geyer, J.R. Jambeck, K.L. Law, Production, use, and fate of all plastics ever made, Sci Adv, 3 (2017) e1700782.

[2] R.C. Thompson, C.J. Moore, F.S. vom Saal, S.H. Swan, Plastics, the environment and human health: current consensus and future trends, Philos Trans R Soc Lond B Biol Sci, 364 (2009) 2153-2166.

[3] H.I. Abdel-Shafy, M.S.M. Mansour, Solid waste issue: Sources, composition, disposal, recycling, and valorization, Egyptian Journal of Petroleum, 27 (2018) 1275-1290.

[4] N.A. Samak, Y. Jia, M.M. Sharshar, T. Mu, M. Yang, S. Peh, J. Xing, Recent advances in biocatalysts engineering for polyethylene terephthalate plastic waste green recycling, Environ Int, 145 (2020) 106144.

[5] S.K. Kale, A.G. Deshmukh, M.S. Dudhare, V.B.J.J.o.B.T. Patil, Microbial degradation of plastic: a review, 6 (2015) 952-961.

[6] F. Kawai, T. Kawabata, M. Oda, Current State and Perspectives Related to the Polyethylene Terephthalate Hydrolases Available for Biorecycling, Acs Sustainable Chemistry & Engineering, 8 (2020) 8894-8908.

[7] A. Biundo, J. Reich, D. Ribitsch, G.M. Guebitz, Synergistic effect of mutagenesis and truncation to improve a polyesterase from Clostridium botulinum for polyester hydrolysis, Sci Rep, 8 (2018) 3745.

[8] E. Bermudez-Garcia, C. Pena-Montes, J.A. Castro-Rodriguez, A. Gonzalez-Canto, A. Navarro-Ocana, A. Farres, ANCUT2, a Thermo-alkaline Cutinase from Aspergillus nidulans and Its Potential Applications, Appl Biochem Biotechnol, 182 (2017) 1014-1036.

[9] E. Herrero Acero, D. Ribitsch, G. Steinkellner, K. Gruber, K. Greimel, I. Eiteljoerg, E. Trotscha, R. Wei, W. Zimmermann, M. Zinn, A. Cavaco-Paulo, G. Freddi, H. Schwab, G. Guebitz, Enzymatic Surface Hydrolysis of PET: Effect of Structural Diversity on Kinetic Properties of Cutinases from Thermobifida, Macromolecules, 44 (2011) 4632-4640.

[10] V. Tournier, C.M. Topham, A. Gilles, B. David, C. Folgoas, E. Moya-Leclair, E. Kamionka, M.L. Desrousseaux, H. Texier, S. Gavalda, M. Cot, E. Guemard, M. Dalibey, J. Nomme, G. Cioci, S. Barbe, M. Chateau, I. Andre, S. Duquesne, A. Marty, An engineered PET depolymerase to break down and recycle plastic bottles, Nature, 580 (2020) 216-219.

[11] E. Herrero Acero, D. Ribitsch, G. Steinkellner, K. Gruber, K. Greimel, I. Eiteljoerg, E. Trotscha, R. Wei, W. Zimmermann, M. Zinn, A. Cavaco-Paulo, G. Freddi, H. Schwab, G. Guebitz, Enzymatic Surface Hydrolysis of PET: Effect of Structural Diversity on Kinetic Properties of Cutinases from Thermobifida, Macromolecules, 44 (2011) 4632-4640.

[12] S. Sulaiman, S. Yamato, E. Kanaya, J.J. Kim, Y. Koga, K. Takano, S. Kanaya, Isolation of a novel cutinase homolog with polyethylene terephthalate-degrading activity from leaf-branch compost by using a metagenomic approach, Appl

Environ Microbiol, 78 (2012) 1556-1562.
[13] C. Roth, R. Wei, T. Oeser, J. Then, C. Föllner, W. Zimmermann, N. Sträter, Structural and functional studies on a thermostable polyethylene terephthalate degrading hydrolase from Thermobifida fusca, Applied Microbiology and Biotechnology, 98 (2014) 7815-7823.
[14] S. Yoshida, K. Hiraga, T. Takehana, I. Taniguchi, H. Yamaji, Y. Maeda, K. Toyohara, K. Miyamoto, Y. Kimura, K. Oda, A bacterium that degrades and assimilates poly(ethylene terephthalate), Science, 351 (2016) 1196-1199.
[15] N.A. Samak, Y.Q. Tan, K.Y. Sui, T.T. Xia, K.F. Wang, C. Guo, C.Z. Liu, CotA laccase immobilized on functionalized magnetic graphene oxide nano-sheets for efficient biocatalysis, Molecular Catalysis, 445 (2018) 269-278.
[16] J. Ge, Biocatalyst and nanocatalyst integrated systems for chemical production, Chin. Sci. Bull., 61 (2016) 3924-3929.
[17] S.S. Nadar, S.D. Gawas, V.K. Rathod, Self-assembled organic-inorganic hybrid glucoamylase nanoflowers with enhanced activity and stability, Int. J. Biol. Macromol., 92 (2016) 660-669.
[18] J. Ge, J. Lei, R.N. Zare, Protein-inorganic hybrid nanoflowers, Nat Nanotechnol, 7 (2012) 428-432.
[19] C. Ke, Y. Fan, Y. Chen, L. Xu, Y. Yan, A new lipase–inorganic hybrid nanoflower with enhanced enzyme activity, RSC Advances, 6 (2016) 19413-19416.
[20] G. Cao, J. Gao, L. Zhou, Y. He, J. Li, Y. Jiang, Enrichment and Coimmobilization of Cofactors and His-Tagged ω-Transaminase into Nanoflowers: A Facile Approach to Constructing Self-Sufficient Biocatalysts, ACS Applied Nano Materials, 1 (2018) 3417-3425.
[21] Y. Song, J. Gao, Y. He, L. Zhou, L. Ma, Z. Huang, Y. Jiang, Preparation of a Flowerlike Nanobiocatalyst System via Biomimetic Mineralization of Cobalt Phosphate with Enzyme, Industrial & Engineering Chemistry Research, 56 (2017) 14923-14930.
[22] Y. Ma, M.D. Yao, B.Z. Li, M.Z. Ding, B. He, S. Chen, X. Zhou, Y.J. Yuan, Enhanced Poly(ethylene terephthalate) Hydrolase Activity by Protein Engineering, Engineering, 4 (2018) 888-893.
[23] L. Rulisek, J. Vondrasek, Coordination geometries of selected transition metal ions (Co^{2+}, Ni^{2+}, Cu^{2+}, Zn^{2+}, Cd^{2+}, and Hg^{2+}) in metalloproteins, J. Inorg. Biochem., 71 (1998) 115-127.
[24] S. Escobar, S. Velasco-Lozano, C.H. Lu, Y.F. Lin, M. Mesa, C. Bernal, F. Lopez-Gallego, Understanding the functional properties of bio-inorganic nanoflowers as biocatalysts by deciphering the metal-binding sites of enzymes, J Mater Chem B, 5 (2017) 4478-4486.
[25] M.S. Ominsky, C. Libanati, Q.T. Niu, R.W. Boyce, P.J. Kostenuik, R.B. Wagman, R. Baron, D.W. Dempster, Journal of Bone and Mineral Research: Volume 30, Issue 5, May 2015, Frontmatter page ii, J Bone Miner Res, 30 (2015) 1347.
[26] R.C. Rodrigues, C. Ortiz, A. Berenguer-Murcia, R. Torres, R. Fernandez-

Lafuente, Modifying enzyme activity and selectivity by immobilization, Chem. Soc. Rev., 42 (2013) 6290-6307.

[27] Z. Li, Y. Ding, S. Li, Y. Jiang, Z. Liu, J. Ge, Highly active, stable and self-antimicrobial enzyme catalysts prepared by biomimetic mineralization of copper hydroxysulfate, Nanoscale, 8 (2016) 17440-17445.

[28] F. Yan, R. Wei, Q. Cui, U.T. Bornscheuer, Y.J. Liu, Thermophilic whole-cell degradation of polyethylene terephthalate using engineered Clostridium thermocellum, Microb Biotechnol, 14 (2021) 374-385.

[29] H.P. Austin, M.D. Allen, B.S. Donohoe, N.A. Rorrer, F.L. Kearns, R.L. Silveira, B.C. Pollard, G. Dominick, R. Duman, K. El Omari, V. Mykhaylyk, A. Wagner, W.E. Michener, A. Amore, M.S. Skaf, M.F. Crowley, A.W. Thorne, C.W. Johnson, H.L. Woodcock, J.E. McGeehan, G.T. Beckham, Characterization and engineering of a plastic-degrading aromatic polyesterase, Proc Natl Acad Sci U S A, 115 (2018) E4350-E4357.

[30] Z. Zhou, Z. Gao, H. Shen, M. Li, W. He, P. Su, J. Song, Y. Yang, Metal-Organic Framework in Situ Post-Encapsulating DNA-Enzyme Composites on a Magnetic Carrier with High Stability and Reusability, ACS applied materials & interfaces, 12 (2020) 7510-7517.

[31] E.T. Hwang, M.B. Gu, Enzyme stabilization by nano/microsized hybrid materials, Engineering in Life Sciences, 13 (2013) 49-61.

[32] K.E. Jaeger, F. Kovacic, Determination of lipolytic enzyme activities, Methods Mol Biol, 1149 (2014) 111-134.

[33] H. Block, B. Maertens, A. Spriestersbach, N. Brinker, J. Kubicek, R. Fabis, J. Labahn, F. Schäfer, Immobilized-metal affinity chromatography (IMAC): a review, Methods Enzymol., 463 (2009) 439-473.

[34] M.S. Kasher, M. Wakulchik, J.A. Cook, M.C. Smith, One-step purification of recombinant human papillomavirus type 16 E7 oncoprotein and its binding to the retinoblastoma gene product, Biotechniques, 14 (1993) 630-641.

[35] Y.J. Chang, C.H. Chang, Protein microarray chip with Ni-Co alloy coated surface, Biosens. Bioelectron., 25 (2010) 1748-1754.

Revised Figures

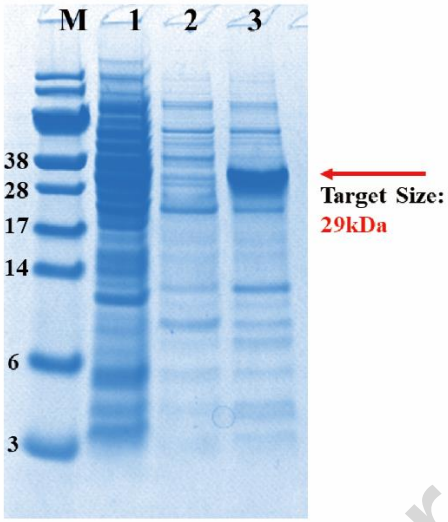

Fig. 1. SDS-PAGE analysis of crude cell lysates containing His-tagged PETase (lane 1) and purified by Ni-NTA affinity chromatography (lane 2) or bionic mineralization process (lane 3). Lane M: protein marker; Lane 4: eluted fractions from the PETase@$Co_3(PO_4)_2$ using 500 mM imidazole. The target protein was marked by a red arrow.

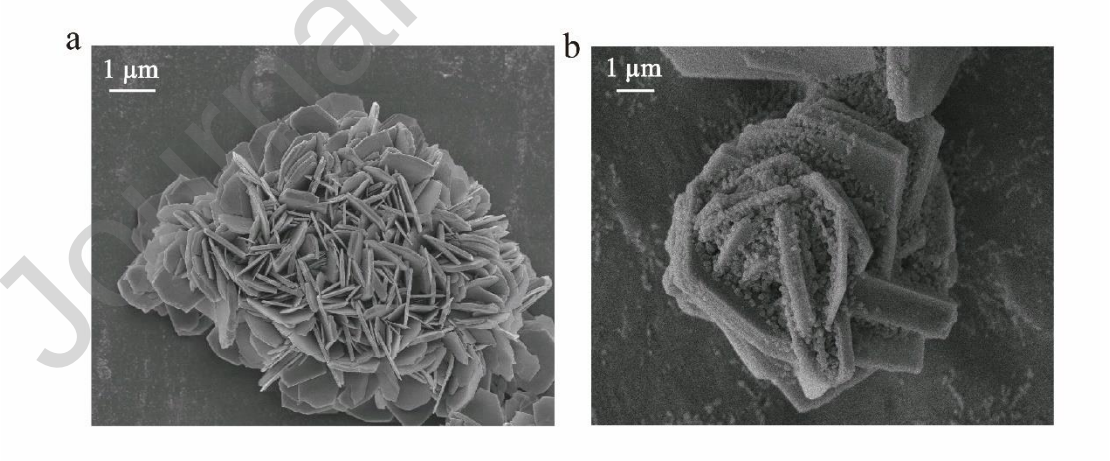

Fig. 2. SEM image of $Co_3(PO_4)_2$ nanoflowers (a) and PETase@$Co_3(PO_4)_2$ (b).

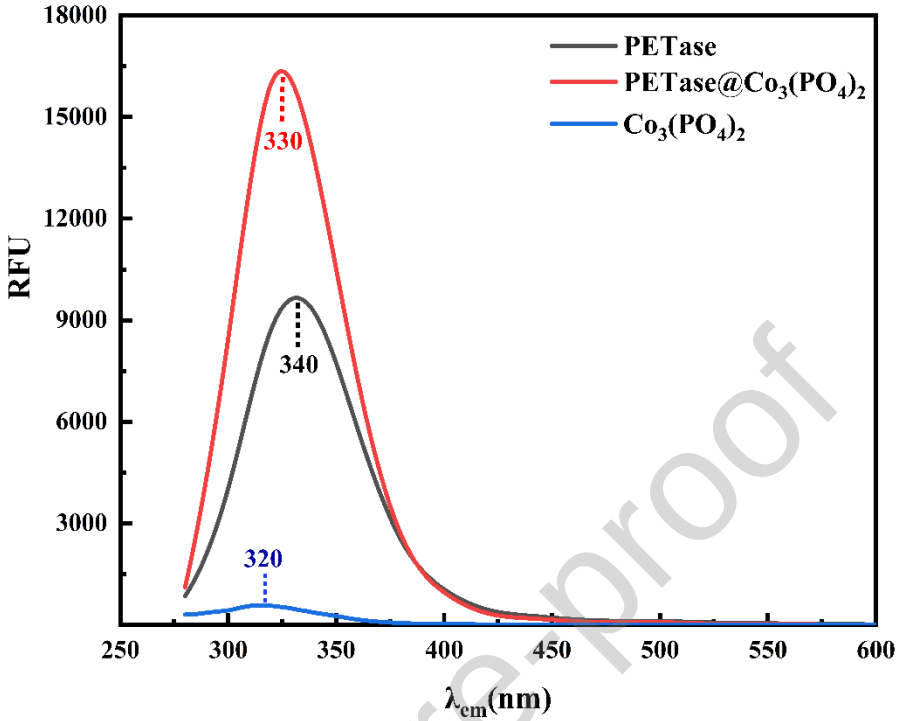

Fig. 3. Fluorescence studies of soluble PETase, PETase@$Co_3(PO_4)_2$ and $Co_3(PO_4)_2$

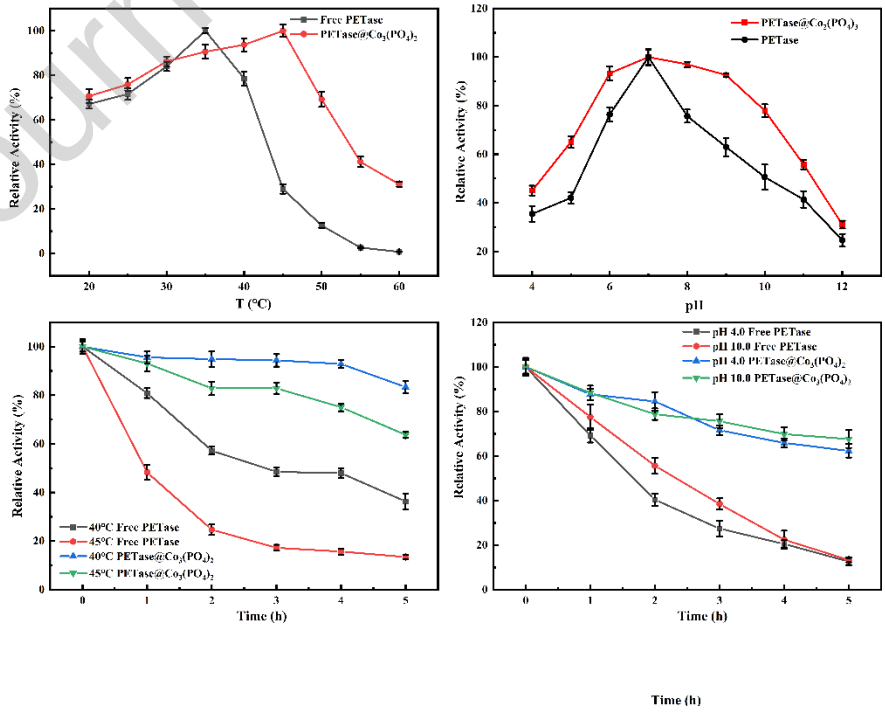

Fig. 4. Optimum temperature(a) and pH (b) of PETase@$Co_3(PO_4)_2$ and free

PETase. Thermal stability(c) and pH stability(d) of PETase@$Co_3(PO_4)_2$ and free PETase

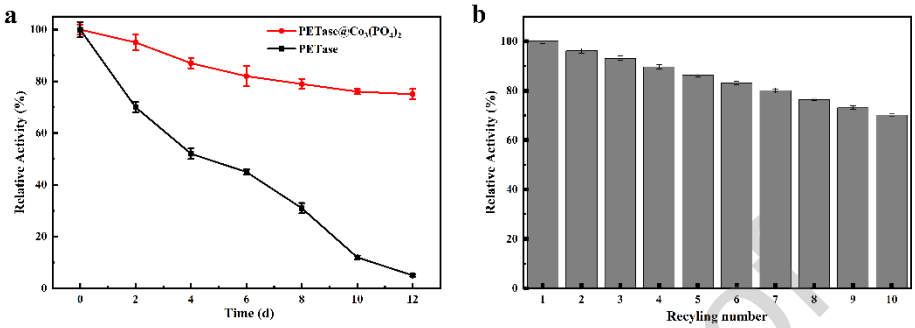

Fig. 5. Storage and reusability results. (a) Storage stability studies of free PETase and PETase@$Co_3(PO_4)_2$ nanoflowers. (b) Reusability of immobilized PETase.

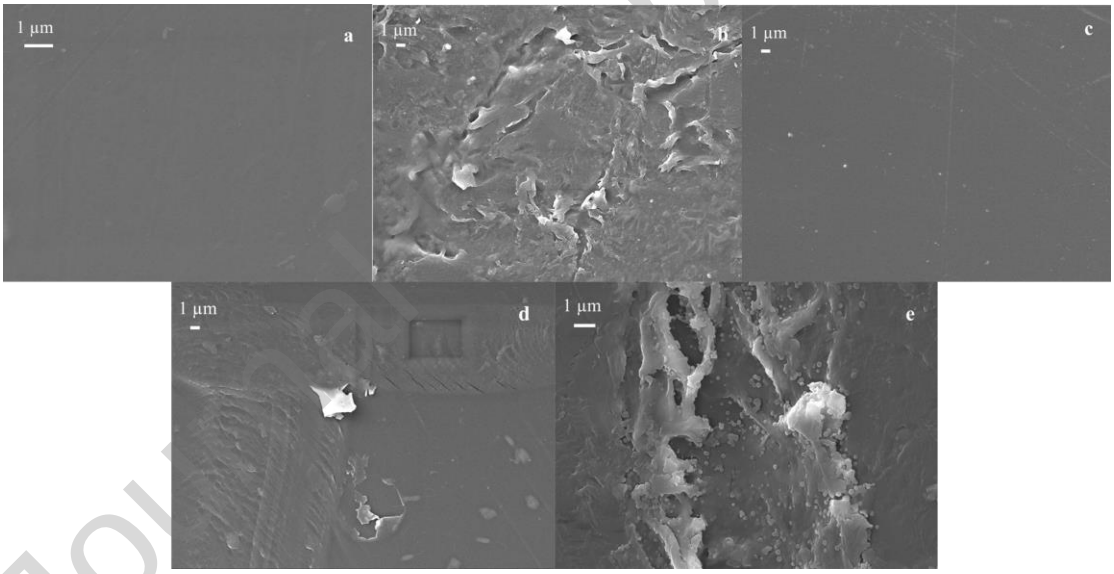

Fig. 6. SEM photographs of bottle-grade PET surface. Untreated (a), treated with PETase@$Co_3(PO_4)_2$ (b) and $Co_3(PO_4)_2$ for 48 h (c), treated with free PETase for 48 h (d), and treated with free PETase for 7 days (e).

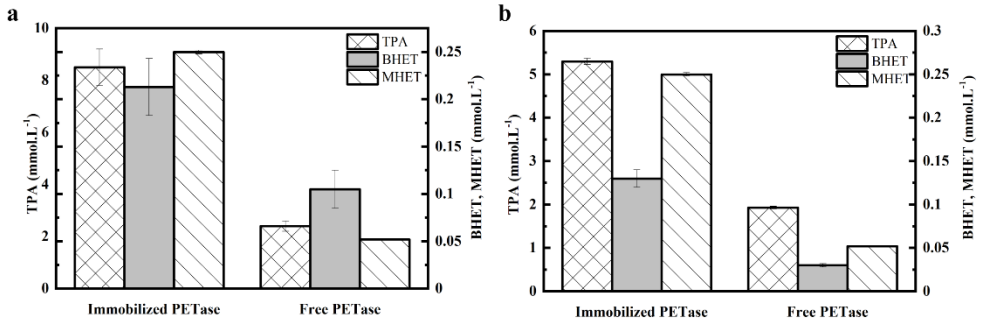

Fig. 7. The hydrolysis products concentration after reacting PETase enzyme and immobilized PETase with PET particles (a) and amorphous PET film (b) for 48 h at 30 °C.

CRediT authorship contribution statement

Yunpu Jia: Conceptualization, Methodology, Validation, Data curation, Writing - Original Draft, Review & Editing. Nadia A. Samak: Methodology, Review & Editing. Xuemi Hao: Review & Editing, Supervision. Zheng Chen: Validation. Gama Yang: Validation. Xuhao Zhao: Validation. Tingzhen Mu: Validation. Maohua Yang: Validation. Jianmin Xing: Conceptualization, Review & Editing, Supervision, Project administration.

Declaration of Competing Interests

☒ The authors declare that they have no known competing financial interests or personal relationships that could have appeared to influence the work reported in this paper.

☐The authors declare the following financial interests/personal relationships which may be considered as potential competing interests:

Graphical abstract

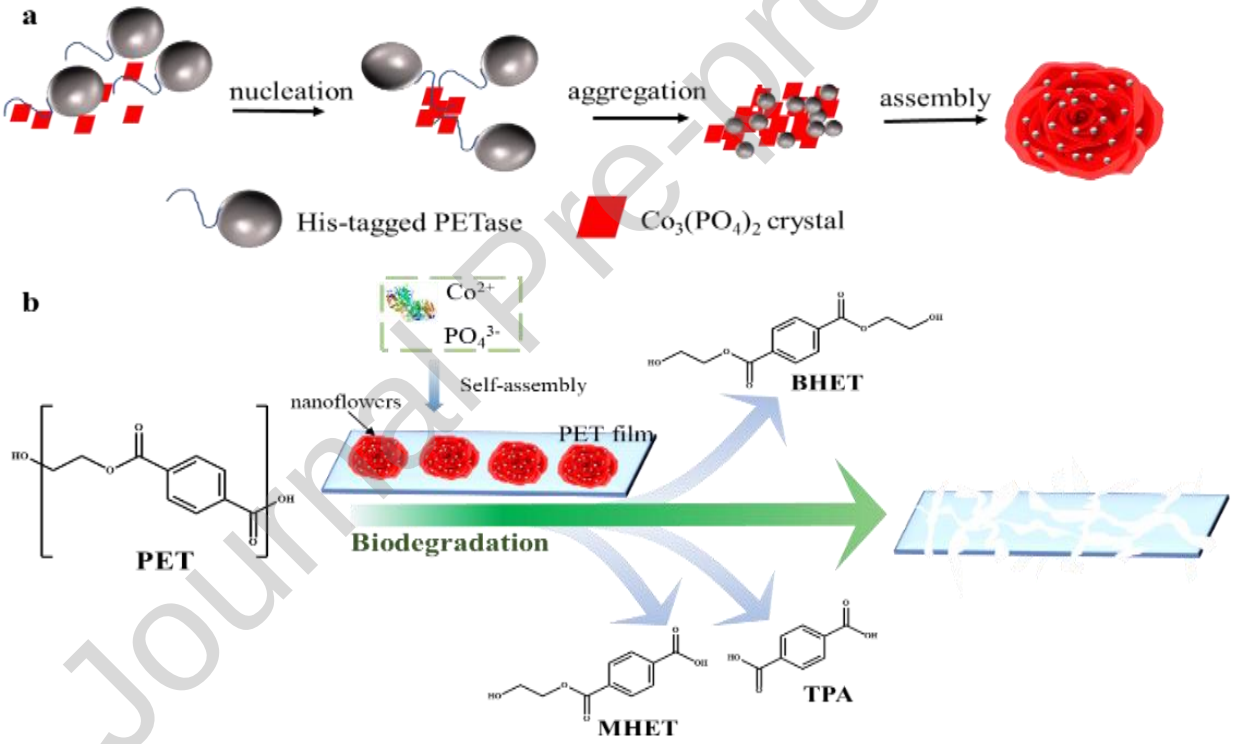

Schematic illustration of PETase@$Co_3(PO_4)_2$ nanoflowers synthesis (a), immobilization of PETase enzyme by biomimetic mineralization, and PET film degradation using the immobilized enzyme(b).

Highlights

- Immobilized PETase was successfully performed via biomimetic mineralization
- The catalytic performance of PETase were enhanced owing to the nano-effect
- The immobilized PETase degraded the surface of PET effectively within two days